Turbulence suppression by active control

Brian F. Farrell
Department of Earth and Planetary Sciences, Harvard University, Cambridge, Massachusetts 02138

Petros J. Ioannou[a)]
Department of Earth and Planetary Sciences, Harvard University, Cambridge, Massachusetts 02138

(Received 19 December 1994; accepted 17 January 1996)

It has recently been recognized that the non-normality of the dynamical operator obtained by the linearization of the equations of motion about the strongly sheared background flow plays a central role in the dynamics of both fully developed turbulence and laminar/turbulent transition. This advance has led to the development of a deterministic theory for the role of coherent structures in shear turbulence as well as a stochastic theory for the maintenance of the turbulent state. In this work the theory of stochastically forced non-normal dynamical systems is extended to explore the possibility of controlling the transition process and of suppressing fully developed shear turbulence. Modeling turbulence as a stochastically forced non-normal dynamical system allows a great variety of control strategies to be explored and their physical mechanism understood. Two distinct active control mechanisms have been found to produce suppression of turbulent energy by up to 70%. A physical explanation of these effective control mechanisms is given and possible applications are discussed. © *1996 American Institute of Physics.* [S1070-6631(96)00405-2]

I. INTRODUCTION

Preventing the transition to turbulence of a laminar flow and suppressing the variance of a turbulent flow, perhaps with the ultimate goal of inducing relaminarization, are in themselves problems of great theoretical and practical importance. In addition, understanding the physical mechanism of turbulence and turbulent transition should lead either to methods of control or to an explanation of why such control is not possible; from this perspective the control problem is seen as a test of physical theory. From the viewpoint of practical engineering, a comprehensive theory of the transition process and of the maintenance of fully developed turbulence that both implied new control mechanisms and provided a means of testing proposed mechanisms would be of great utility, even if the result were to discourage the search for, e.g., a passive compliant membrane that relaminarized the turbulent boundary layer. Extensive attempts to reduce drag in turbulent boundary layer flow by imposing a variety of active and passive control measures have shown that in the absence of applicable theory it is very unlikely that an optimal method can be identified.[1]

The control problem is made more difficult by the fact that there are no results available on the structure of the domain of attraction of the laminar flow for subcritical Reynolds numbers in shear flow (at least for Reynolds numbers in excess of those for which the laminar solutions are universally attracting, i.e. $R=20.7$ for Couette flow, $R=49.6$ for plane Poiseuille). However, there is ample experimental evidence that sufficiently small perturbations fail to induce transition, at least for $R<10^5$. This observation suggests that a control strategy that adequately suppresses the perturbation variance will succeed in maintaining the laminar flow. Unfortunately the exact degree of perturbation suppression needed to keep the flow laminar is not known theoretically (as such knowledge would be tantamount to knowing the structure of the domain of attraction). Because of this limitation in our knowledge, proposed strategies can only be verified by actual experiment or by direct numerical simulation.

A widely accepted theory of transition envision exponentially unstable two dimensional T–S waves growing as exponential instabilities until falling victim to secondary three-dimensional instabilities, which, in turn, give way to a cascade of further instabilities with the ensemble of these exponential instabilities supporting the turbulent state.[2] Control strategies proceeding from this paradigm include attempts to lower the growth rate of the primary unstable T–S wave by using suction to change the velocity profile[3] and by altering the viscosity of the flow through heating or cooling the surface,[4] in addition to attempts to depress growth rates using compliant boundaries[1,5,6] and direct active cancellation of the T–S waves by introduction of antiphase perturbations.[7]

The assumption that modal instabilities leading to transition are necessarily two dimensional apparently follows from Squire's theorem,[8] which requires the maximally growing inviscid modal instability to be two dimensional and is commonly interpreted to imply a similar restriction in viscous flow. However, observation reveals an important role for three-dimensional disturbances in transition and the perturbations exhibiting greatest growth can be shown to be both nonmodal and three dimensional.[9,10]

While exponential instability theory provides a plausible explanation for transition in which the unstable T–S waves grow initially as modal waves and in which these unstable waves can be addressed for the purposes of control by cancellation or by intervention to reduce their growth rates, modal instability theory provides much less guidance toward affecting control of fully developed turbulence for which a useful correspondence between unstable modes and observed

[a)]Corresponding author: Telephone: (617)-496-2410; electronic mail: pji@io.harvard.edu

coherent structures has not been found. For this reason attempts to effect control based on exponential instability theory have been confined to delaying transition by suppressing T–S waves in nonbypass transition.

Recently, an alternative theory has been advanced based on the great potential of a subset of perturbations to increase in energy by transient growth processes unrelated to the existence of exponential instabilities.[9–15] Moreover, this theory of transient growth in non-normal dynamical systems has recently been extended to provide a theory for the maintenance of the turbulent state in which the growing subset of perturbations that are replenished by spectral transfer in the fully nonlinear system,[16] are instead replenished by a parametrized stochastic forcing in the model.[17,18]

The problem of inhibiting transition is necessarily linear if free-stream perturbations are constrained to be sufficiently small, and in this limit the linear non-normal transient growth mechanism necessarily underlies transition in flows without robust exponential instabilities, including the canonical Couette, pipe Poiseuille, plane Poiseuille (below Reynolds number 5772), and exponentially stable boundary layer flows—all of which exhibit bypass transition. In the case of plane Poiseuille flow and Blasius flow at Reynolds numbers for which unstable T–S waves exist, the growth rate of the exponential instability is small compared with that of the subset of rapidly growing three-dimensional perturbations, so that even in these cases the unstable growth of T–S waves is unlikely to be important, except under carefully controlled experimental conditions designed to forestall bypass transition.

From the theoretical perspective of transient development in non-normal dynamical systems, suppressing transition requires inhibiting the development of nonmodal perturbations with the potential for growth. It is obvious that if the entire perturbation field were observed and that if the control were able to address the entire field, then complete cancellation would be possible. It is not so obvious that observation of a single variable at a cross-stream plane coupled with control of a single variable at the surface would be sufficient to suppress the growth of perturbations throughout the boundary layer.

As is the case for inhibiting transition to turbulence, reducing the variance in fully developed turbulence also requires intervention to suppress the growing subset of coherent structures. Again, it is not immediate that observation and control, in which each is confined to a single variable at a single cross-stream level, can be effective. The method that will be used to study this problem is to construct a parametrized model of the turbulent flow by stochastically forcing the associated non-normal dynamical system linearized about the background shear flow followed by imposition of control in this model. Because the coherent structures dominating, the energetics of the turbulent state can be identified with the dominant optimal perturbations arising from the non-normal dynamical operator[10,19] it follows that suppression of these variance producing structures in the linear parametrized turbulence model should at least provide guidance in the choice of control strategies for fully turbulent flow.

The stochastic model of turbulence we are using fails to reproduce the full complexity of turbulence observed in shear flow. This model cannot substitute for direct numerical simulation of a turbulent flow, which can be expected to provide a more realistic model of turbulence. However, for the purposes of evaluating control strategies a turbulence model need only provide an adequate approximation to the development of the coherent structures primarily responsible for the energetic interaction between the mean flow and the perturbation field. Because the non-normal operator includes this interaction while retaining the simplicity of a linear operator it is the least complex turbulence model retaining the essential physics underlying the maintenance of perturbation variance.

Some advantages of the method of analyzing turbulence control strategies outlined here are that it facilitates testing a wide variety of mechanisms and provides physical insight into their method of operation. Of great interest are simple local reactive controls that do not require identification of a wave and subsequent cancellation at a downstream point but rather require only a rule specifying the local response in some variable to an observation of another or perhaps the same variable. Such controls could potentially be implemented using a simple local feedback loop.

An example of such a feedback control in a fully nonlinear turbulent flow simulation has been described by Choi *et al.*[20] These authors observed the cross-stream normal velocity at various distances from the wall and imposed an equal normal velocity control at the wall. For an observing distance measured in wall units of $y^+=10$, they obtained a 30% suppression of mean drag, and in some instances succeeded in relaminarizing the flow. However, for other observing distances increases of variance were found. Comparison will be made between the results of Choi *et al.*[20] and predictions based on the control theory developed in this work.

II. FORMULATION OF THE CONTROL PROBLEM

A. Implementing active boundary control in the dynamical operator

Consider the evolution of small perturbations imposed on a steady channel flow with streamwise (x) background velocity $U(y)$ varying only in the cross-stream direction (y). Harmonic perturbations with streamwise wave number k and spanwise (z) wave number l obey the linear equation:

$$\frac{d\phi}{dt}=\mathcal{B}\phi, \tag{1}$$

where the state variable is $\phi=[\hat{v},\hat{\eta}]^T$, in which $\hat{v}$ is the cross-stream perturbation velocity, and $\hat{\eta}=il\hat{u}-ik\hat{w}$ is the cross-stream perturbation vorticity ($\hat{u},\hat{w}$ are the perturbation streamwise and spanwise velocities, respectively). The dynamical operator in (1) is obtained from the linearized Navier–Stokes equations by eliminating the pressure field using the continuity equation.[21] The operator is given by

$$\mathcal{B}=\begin{bmatrix}\mathcal{L} & 0\\ \mathcal{C} & \mathcal{S}\end{bmatrix}, \tag{2}$$

with

$$\mathscr{S}=\Delta^{-1}(-ikU\Delta+ikU''+\Delta\Delta/R), \tag{3a}$$

$$\mathscr{S}=-ikU+\Delta/R, \tag{3b}$$

$$\mathscr{C}=-ilU', \tag{3c}$$

in which the Laplacian operator is given by $\Delta\equiv d^2/dy^2-K^2$, with K being the total horizontal wave number: $K^2=k^2+l^2$. Cross-stream derivatives of the mean fields are denoted with a dash. The equations have been rendered nondimensional with the maximum background velocity in the channel, U_0, and the channel half-width, L, so that the Reynolds number is $R\equiv U_0L/\nu$; ν denoting the kinematic viscosity. A well-posed inversion of the Laplacian in (3a) requires incorporating the boundary conditions at the channel walls $y=\pm1$.

The components of the dynamical operator (2) are the Orr–Sommerfeld operator, $\mathscr{S}$, the coupling operator between cross-stream velocity and vorticity, $\mathscr{C}$, which corresponds physically to the generation of cross-stream vorticity by tilting of the mean spanwise vorticity; and the advection-diffusion Squire operator, $\mathscr{S}$. In the numerical calculations that follow all continuous operators are approximated by finite differences, rendering the continuous dynamical system finite dimensional. Accuracy is checked by doubling the resolution of the discretization.

We choose to impose symmetric control at the channel walls $y=\pm1$ in reaction to observations of a field variable at $Y_1^{\rm ob}=-1+Y_0$ and at $Y_2^{\rm ob}=1-Y_0$. By cross-stream velocity control we mean that observations of the cross-stream velocity at $Y_1^{\rm ob}, Y_2^{\rm ob}$ are used to impose a cross-stream velocity at $y=\pm1$ according to

$$\begin{aligned}\hat{v}(-1)&=C\hat{v}(Y_1^{\rm ob}),\\ \hat{v}(1)&=C\hat{v}(Y_2^{\rm ob}),\end{aligned} \tag{4}$$

where C is a complex control constant. Clearly, alternative controls can be imposed in a similar manner.

The remaining boundary conditions for the case of active specification of the cross-stream ($\hat{v}$) velocity at the boundaries are the vanishing of the streamwise ($\hat{u}$) and spanwise velocity ($\hat{w}$) components, which requires at the walls

$$\begin{aligned}\hat{u}&=-\frac{i}{K^2}\left(l\hat{\eta}-k\frac{d\hat{v}}{dy}\right)=0,\\ \hat{w}&=\frac{i}{K^2}\left(k\hat{\eta}+l\frac{d\hat{v}}{dy}\right)=0.\end{aligned} \tag{5}$$

Consequently, at the channel wall we have the following boundary conditions:

$$\begin{aligned}\left.\frac{d\hat{v}}{dy}\right|_{y=\pm1}&=0,\\ \hat{\eta}(\pm1)&=0.\end{aligned} \tag{6}$$

Note that the perturbation evolution equation (1) together with boundary conditions (4) and (6) form a linear system with homogeneous boundary conditions and that imposition of feedback control constitutes a change in the boundary conditions of the flow. Therefore the control action cannot be understood using arguments about cancellation or reinforcement of perturbations that exist in the unmanipulated flow. Instead, suppression of turbulence occurs because control parameters alter the boundary conditions so as to constrain the perturbations to exhibit reduced growth compared to that found with the standard boundary conditions in the unmanipulated flow.

As an aid to interpreting the control action, we form the perturbation energy equation,

$$\frac{dE}{dt}=\int_{-1}^{1}dy\left(U\frac{d\overline{uv}}{dy}-\frac{1}{R}\overline{(u\ \Delta u+v\ \Delta v+w\ \Delta w)}\right)-\overline{pv}|_{y=1}+\overline{pv}|_{y=-1}, \tag{7}$$

where the overbar denotes integration over a single period in the horizontal (x,z) plane. The Reynolds stress is related to the Fourier amplitudes by $\overline{uv}=1/2\ \mathrm{Re}(\hat{u}\hat{v}^*)$, and the perturbation kinetic energy is given by

$$E=\frac{1}{2}\int_{-1}^{1}dy\ \overline{u^2+v^2+w^2}. \tag{8}$$

The first term on the rhs of (7) can be interpreted in the integral sense as the rate of change of energy arising from the local acceleration of the mean flow by divergence of the perturbation Reynolds stress, the second term is the dissipation due to viscous diffusion, and the two boundary terms represent energy injection at the boundaries, which may be nonzero when a control action is applied. The pressure at the wall is given by

$$\hat{p}(\pm1)=\frac{ik}{K^2}U'(\pm1)\hat{v}(\pm1)+\frac{1}{RK^2}\left.\frac{d^3\hat{v}}{dy^3}\right|_{y=\pm1}. \tag{9}$$

We will determine the magnitude and phase of the control C and the observation level Y_0 that reduces the growth of perturbations. Plane Poiseuille flow with $U=1-y^2$ and a Reynolds–Tiederman boundary layer flow are used for the examples.

B. Estimating the growth of perturbations under active boundary control

In order to proceed it is necessary to have a measure of perturbation growth. We choose the perturbation energy given in operator form by

$$E=\phi^\dagger\mathscr{M}\phi. \tag{10}$$

In (10) $\phi^\dagger$ is the Hermitian transpose of ϕ and the energy metric is defined, for a cross-stream grid δy, by

$$\mathscr{M}=\frac{\delta y}{8K^2}\begin{bmatrix}-\Delta & 0\\ 0 & I\end{bmatrix}, \tag{11}$$

where I is the identity and Δ is the finite difference approximation of the corresponding continuous operator, which has been rendered invertible by incorporation of the boundary conditions.

We transform (1) into generalized velocity variables $\psi=\mathscr{M}^{1/2}\ \phi$ so that the usual L_2 norm corresponds to the square root of the mean energy. Under this transformation a perturbation ψ_0 at $t=0$ evolves to time t according to

$$\psi^t = e^{\mathscr{A}t}\psi_0, \tag{12}$$

in which the dynamical operator has been transformed to the similar $\mathscr{A}=\mathscr{M}^{1/2}.\mathscr{B}.\mathscr{M}^{-1/2}$.

The energy at t is given by $E^t = \psi_0^\dagger e^{\mathscr{A}^\dagger t} e^{\mathscr{A}t}\psi_0$. The optimal perturbation[9,11] giving the maximum possible growth at t is the eigenvector that corresponds to the greatest eigenvalue of $e^{\mathscr{A}^\dagger t}e^{\mathscr{A}t}$. Equivalently,[14,15] this optimal growth is given by the square of the spectral norm of $\|e^{\mathscr{A}t}\|$, which is equal to the maximum singular value of $e^{\mathscr{A}t}$. This energy growth is due to the non-normality of the evolution operator (i.e., $\mathscr{A}.\mathscr{A}^\dagger \neq \mathscr{A}^\dagger.\mathscr{A}$), and has been recently demonstrated[9–15] to obtain values $O(R^2)$. The transiently growing optimal perturbations can be identified with the characteristic coherent structures (streaks near the wall, double rollers farther from the wall), which are responsible both for bypass transition and for maintenance of the variance in turbulent flow.[10,19]

An alternative measure of growth at time t is the square of the Frobenius norm of $e^{\mathscr{A}t}$. This quadratic measure is equal to the sum of the squares of the singular values of $e^{\mathscr{A}t}$. This measure is proportional to the growth over an interval t of the mean perturbation when all perturbations are forced equally initially. The time integral of this measure is proportional to the perturbation variance maintained in the channel flow under white noise forcing, i.e. the accumulated variance over an interval t for unit forcing of each degree of freedom is given by

$$\langle E^t \rangle = \mathrm{trace}\left(\int_0^t e^{\mathscr{A}t} e^{\mathscr{A}^\dagger t}\, dt \right), \tag{13}$$

where the brackets denote ensemble averaging. The steady-state maintained variance $\langle E^\infty \rangle$ is given for asymptotically stable systems as the limit of (13) as $t\to\infty$.

Due to the non-normality of the evolution operator, the variance cannot be obtained by summing the responses of the individual modes, as in a normal system, and indeed for all stable non-normal dynamical systems,[22]

$$\langle E^\infty \rangle > \sum_{i=1}^{N} \frac{1}{-(\lambda_i + \lambda_i^*)}, \tag{14}$$

where λ_i are the eigenvalues of $\mathscr{A}$ and N is the dimension of the system. The sum on the rhs of (14) is the variance that would result if the operator $\mathscr{A}$ were a normal operator with the same spectrum as $\mathscr{A}$, in which case the maintained variance for unit forcing of each degree of freedom is well known to be the sum of the inverse of twice the decay rates of the individual modes.[23]

The maintained variance for asymptotically stable flows is found by solving the Lyapunov equation for the correlation matrix[17] V^∞:

$$\mathscr{A}V^\infty + V^\infty \mathscr{A}^\dagger = -I, \tag{15}$$

with $V_{ij}^{00} = \langle \psi_i \psi_j^* \rangle$ and I the identity matrix corresponding to unitary forcing. The asymptotic variance can be identified with the trace of the correlation matrix, $\langle E^\infty \rangle = \mathrm{trace}(V^\infty)$. Moreover, eigenalysis of the Hermitian and positive definite correlation matrix V^∞ yields the Empirical Orthogonal Functions (EOF) decomposition of the variance. The first EOF for the unmanipulated flow is shown in Fig. 1. Note that the streaks are centered at a distance of approximately $y=0.5$ from the walls.

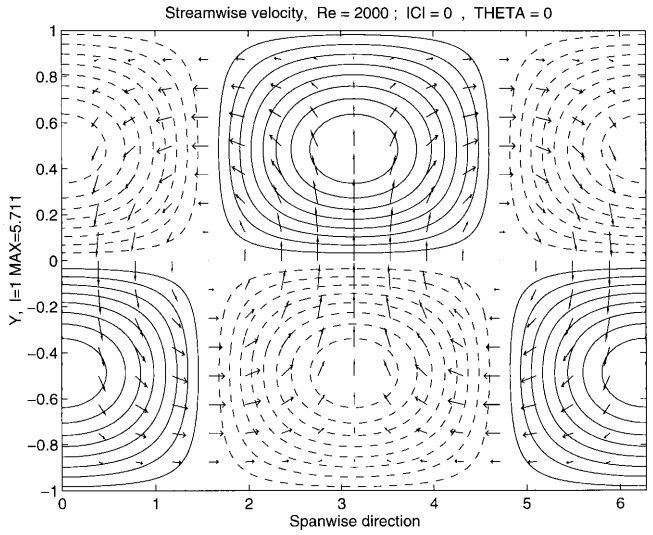

FIG. 1. Contours of the streamwise velocity distribution in the $y-z$ plane for the first EOF accounting for 63% of the total eddy energy. The perturbations are rolls ($k=0$) with total wave number $K=l=1$. The mean flow is Poiseuille and the Reynolds number is $R=2000$. There is no control applied. The plotted vectors are the projection of the velocity vector on the $y-z$ plane. Note that the streaks are located at $y=0.5$ (in fully turbulent flows the corresponding streaks are located at a distance of 20–30 wall units from the boundaries).

The variance maintained by unbiased forcing in an unmanipulated Poiseuille flow peaks at the roll axis ($k=0$) and has for $R=2000$ a broad maximum at $K=O(1)$, as shown in Fig. 2. For large Reynolds number ($R>1000$), the peak wave number increases linearly with Reynolds number. Oblique harmonic perturbations also build energetic streaks and maintain substantial variance.[17,18] Consequently, in our investigation of optimal control parameters we include oblique perturbations.

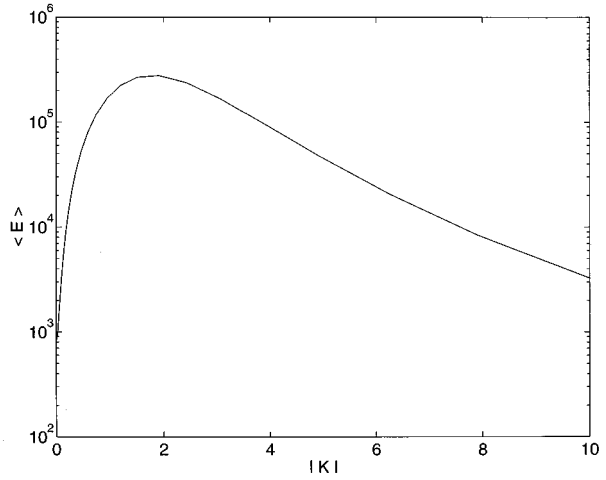

FIG. 2. Ensemble average energy $\langle E \rangle$ for roll perturbations ($k=0$) as a function of total wave number $K=l$.

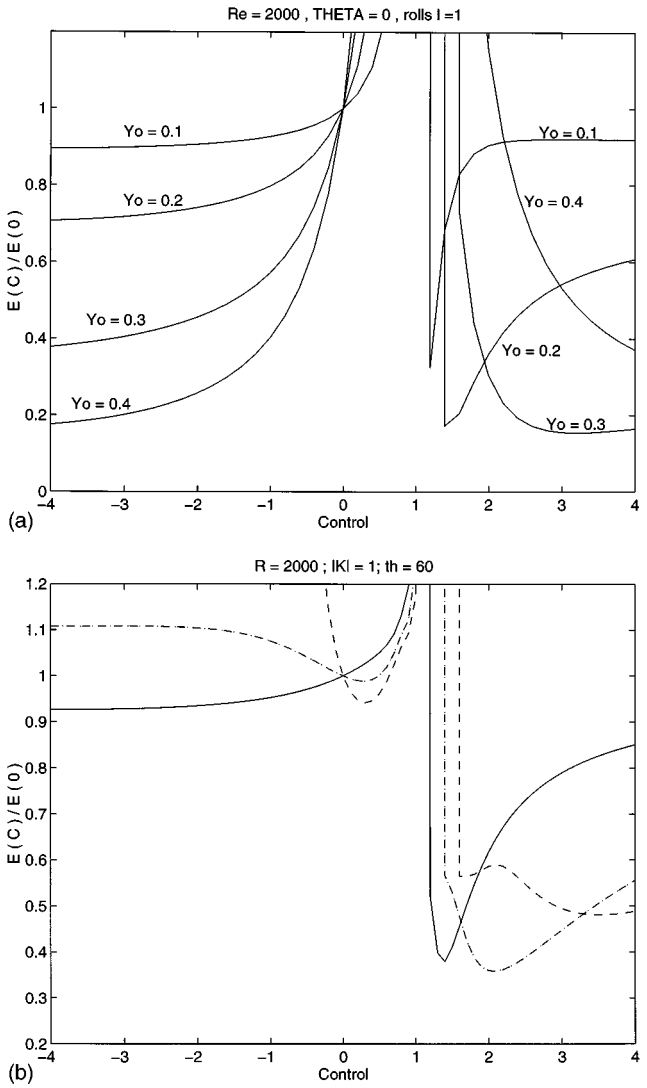

FIG. 3. (a) Suppression of variance of roll perturbations ($k=0$, $\theta=90°$) as a function of the magnitude of the cross-stream velocity control at the walls for various observation distances Y_0 from the wall. Positive control values correspond to in phase control, negative control values correspond to out of phase control. The total wave number is $K=l=1$ and the Reynolds number is $R=2000$. (b) Suppression of the variance of oblique perturbations [with $\theta=60°$, recall $k=K\cos(\theta)$] as a function of the magnitude of the cross-stream velocity control imposed at the walls for various observation distances Y_0 from the wall. Positive control values correspond to in phase control, negative control values correspond to out of phase control. The total wave number is $K=l=1$ and the Reynolds number is $R=2000$. The continuous line is for observation at $Y_0=0.1$, the dot–dashed line for $Y_0=0.2$, and the dashed line for $Y_0=0.3$.

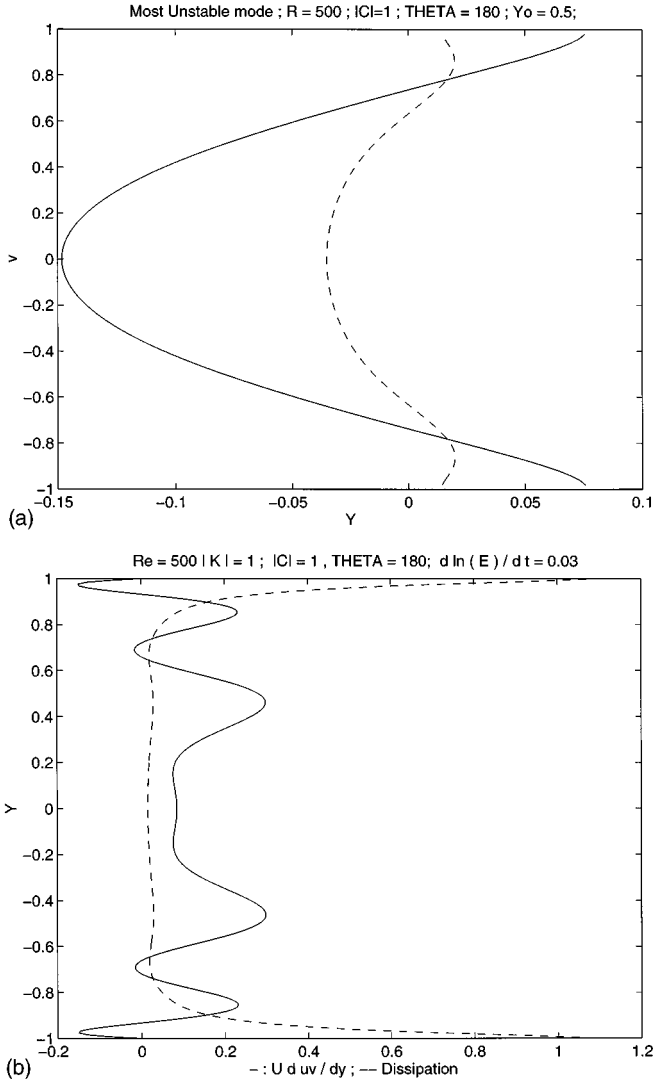

FIG. 4. (a) The structure of the cross-stream velocity (real part continuous line, imaginary part dashed line) for the most unstable mode (growth rate 0.015) with $R=500$, and for a perturbation with $\theta=0°$ and total wave number $K=k=1$. The control is out of phase and has unit amplitude. The observations are at $Y_0=0.5$. (b) The associated energy conversions. The continuous line is $U\overline{du\,v}/dy$ and the dashed line is the dissipation. The boundary energy source is destabilizing and contribute to approximately half of the energy delivered by the Reynolds stress.

The stochastic theory of turbulence outlined above has recently been applied to obtain the energy containing structures of turbulent boundary layers, and particularly to recover the leading EOF of the turbulent boundary layer, which consists of streaks near the walls with peak streamwise velocity at approximately 25 wall units and spanwise spacing of 100 wall units. The same theory also reproduced the observed frequency–wave number spectra. Because of the universality of the dynamics producing coherent structures in shear flows, we expect that control strategies will display a similar generality in fully turbulent flows.

Effective controls, C, are those that minimize

$$\frac{\langle E_C^{\infty}\rangle}{\langle E_0^{\infty}\rangle}, \tag{16}$$

in the complex C plane, where $\langle E_0^{\infty}\rangle$ is the variance maintained under stochastic forcing with no control applied ($C=0$). We investigate the magnitude of the variance suppression as a function of the amplitude $|C|$ and phase Θ of the control for roll and oblique perturbations and for observation at various distances from the wall, Y_0. An effective control must lead to robust suppression of both roll and oblique perturbations.

III. IN PHASE AND OUT OF PHASE CONTROL

We first constrain the control parameter to be real. The variance suppression for in phase ($C>0$) and out of phase control ($C<0$) is shown in Figs. 3(a) and 3(b) for roll and a

typical oblique perturbation.

As expected, in phase control leads for small control amplitudes to increased variance, and in the vicinity of $C=1$ the flow becomes unstable. Remarkably, for higher amplitudes and with observation levels sufficiently near the wall robust variance suppression is found. This mechanism will be referred to as overdriving suppression.

The instability in the vicinity of $|C|=1$ arises from the diffusion term and the boundary condition $d\hat{v}/dy=0$ at the wall. This instability occurs in the absence of flow, as can be readily checked by calculating the spectrum of the Orr–Sommerfeld operator (3a) with $U=0$, so that only the diffusion term is present. Unlike shear instabilities, which are stabilized for sufficiently small Reynolds numbers, this diffusive instability can be shown by a scaling argument to persist for all nonzero Reynolds numbers. For the fourth-order Orr–Sommerfeld operator the diffusive instability vanishes for sufficiently large control amplitude. For second-order diffusion operators, such as that govern heat conduction, the instability can be shown to persist for all control amplitudes larger than the threshold. It can be shown that in phase control of these diffusive operators result in an enhancement of variance in the parameter range in which they are are asymptotically stable.

In contrast to the enhancement of variance resulting from in phase control of the Orr–Sommerfeld operator with $U=0$, the presence of shear can lead to suppression of variance for this operator at sufficiently large Reynolds numbers and large control amplitudes. This overdriving suppression is a consequence of the non-normality of the advection term in the Orr–Sommerfeld operator and cannot be understood as arising from the diffusive term.

It can be seen from Figs. 3(a) and 3(b) that in phase overdriving at an amplitude $C\approx 2$ leads to variance suppression of the order of 60%–70% when observations are made at $Y_0=0.2$ from the wall. This control robustly suppresses the variance of both roll and oblique perturbations.

Out of phase control of roll perturbations leads to robust reduction of variance with the suppression becoming more effective the farther the observation level is located from the controlled boundary (at least for $Y_0<0.5$). Maximum suppression requires amplitudes $|C|>4$. Greater observing distances Y_0, not shown in Fig. 3(a), lead to a minimum associated with a 90% variance suppression for control amplitudes $|C|\approx 1$. Unfortunately, this promising control strategy does not generalize to oblique perturbations, as is evident in Fig. 3(b), which shows the variance for a perturbation with phase lines at an angle $\theta=60°$ to the spanwise direction $[k=K\cos(\theta),\ l=K\sin(\theta)]$. For $Y_0>0.2$ and with out of phase control of amplitude $|C|\approx 1$, oblique perturbations become unstable, leading to variance increase. This instability appears at low Reynolds numbers [typically $R=O(500)$] and analysis of the energetics of the instability reveals that the control injects only a small amount of energy while the predominant energy source is the down-gradient Reynolds stress term. The most unstable perturbations occur at $\theta=0$, in agreement with predictions of Squire's theorem. The analysis of the most unstable 2-D perturbation ($\theta=0$) at $R=500$ with unit out of phase control amplitude and observation at $Y_0=0.5$ is shown in Fig. 4(a) and analysis of the energetics is shown in Fig. 4(b).

The direct numerical simulation experiments of Choi *et al.*[20] showed that out of phase control of unit amplitude ($C=-1$) leads to drag reduction for observations at locations less than 20 wall units and to drag increase for observations at greater distances from the wall. The cause of this drag increase is presumably inception of the instability described above. To check this a stability calculation was performed on the symmetric mean velocity profile proposed by Reynolds and Tiederman:[24]

$$U(y)=\int_{-1}^{y} dy\ \frac{Ry}{1+\nu_E(y)},\quad \text{for } y\in[-1,1], \tag{17}$$

in which the variable eddy viscosity is given by

$$\nu_E(y)=\frac{\{1+[(1/3)\kappa R(1-y^2)(1+2y^2)(1-e^{-(1-|y|)R/A})]^2\}^{1/2}-1}{2}, \tag{18}$$

in terms of a von Kármán constant κ and a boundary thickness parameter A that characterizes the thickness of the wall region velocity variation in Van Driest's wall law. This profile reproduces the mean velocity of turbulent channel flows for a wide range of Reynolds numbers. The Reynolds–Tiederman velocity profile for $\kappa=0.525$, $A=37$, and for a Reynolds number (based now in the friction velocity) of $R=180$ is shown in Fig. 5. The results of the stability analysis of the Orr–Sommerfeld operator for this profile (shown in Fig. 6) indicates that inception of the instability occurs for observations located at 30 wall units (for this Reynolds number a wall unit is related to the nondimensional length by $y^+=180y$ so 30 wall units corresponds to $y=0.17$).

The calculations reported here and the experiments of Choi *et al.*[20] were carried out in a channel flow so that the possibility remains that the instability occurring in the vicinity of out of phase control ($\Theta=180$) would not occur in boundary layer flows. To check this, a stability analysis was performed on the one-sided Reynolds–Tiederman profile. Although the instability occurs at a higher value of observation locations (for observations located at 40 wall units from the boundary) it is qualitatively similar to that found in channel flow. The possibility of maintaining stability at higher observation levels in boundary layer flows suggests that greater suppression of turbulence could be achieved by out of phase control in the boundary layer.

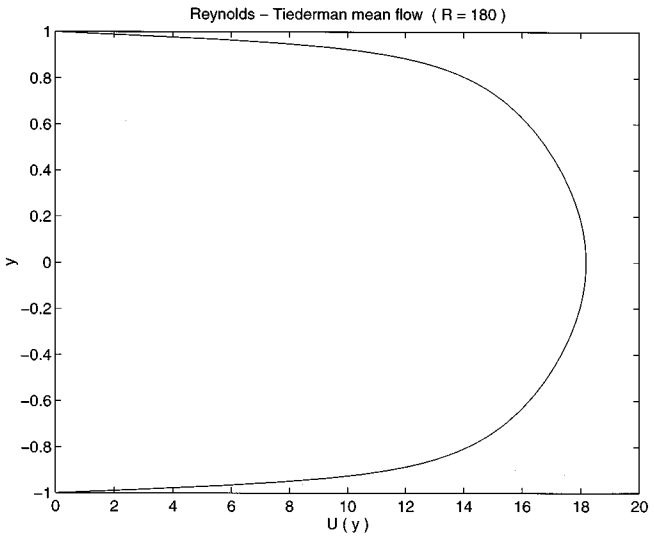

FIG. 5. The Reynolds–Tiederman profile. The Reynolds number based on the friction velocity is $R=180$.

IV. CONTROL OF ROLL PERTURBATIONS

We first consider control actions in which the boundary response is in quadrature with the observation ($\Theta=\pm 90°$). For roll perturbations ($\theta=90°$), a robust suppression of variance as a function of the control amplitude is found for various observation levels $Y_0<0.4$ [Fig. 7(a)]. For $Y_0=0.4$ the variance suppression can reach 70%–80% for control amplitudes $|C|\approx 4$. For observation levels $Y_0>0.5$ roll perturbations show an increase in variance for $\theta=90°$ [Fig. 7(b)].

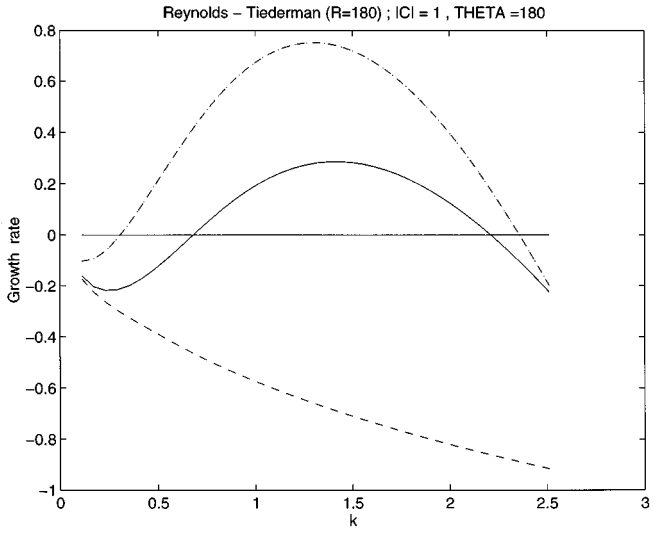

FIG. 6. Growth rate of the most unstable wave as a function of streamwise wave number for various observation distances Y_0 from the wall for out of phase control of unit magnitude ($|C|=1$, $\Theta=180°$). The mean flow is Reynolds–Tiederman with $R=180$. The dashed line is for observations a distance 20 wall units from the boundary ($y=0.11$), the continuous line is for a distance of 30 wall units ($y=0.167$), and the dash–dotted line for observation at 40 wall units ($y=0.22$). Growth rates are here nondimensionalized by L/U_τ, where U_τ is the friction velocity.

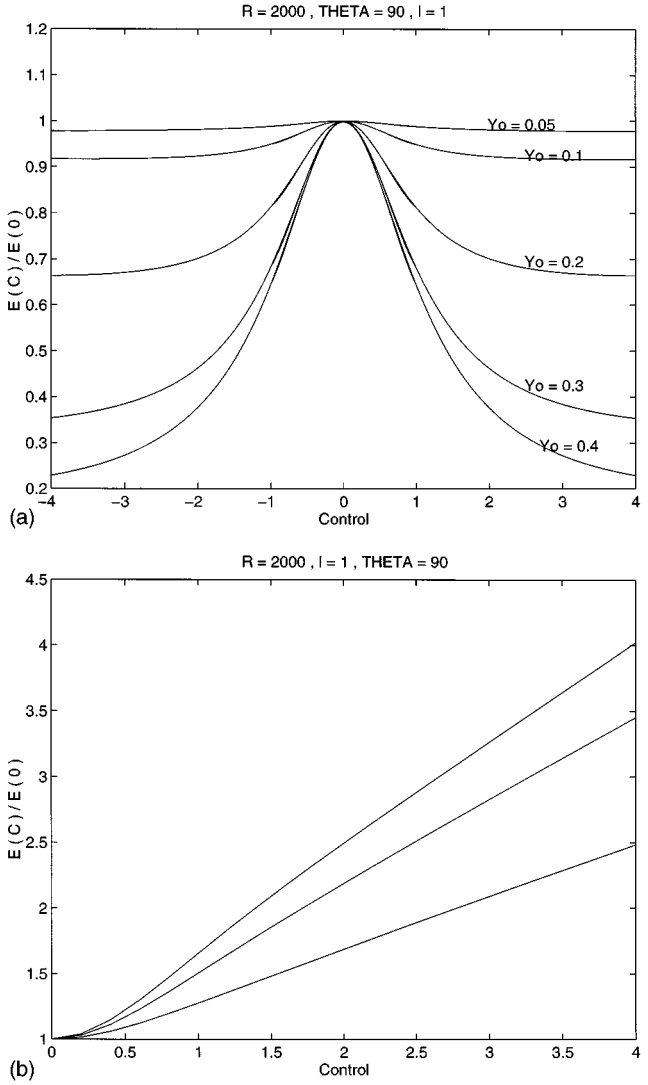

FIG. 7. (a) Suppression of variance for roll perturbations ($k=0$, $\theta=90°$) as a function of the magnitude of the cross-stream velocity control at the walls and for various observation distances Y_0 from the wall. Positive controls correspond to controls with phase $\Theta=90°$, negative controls correspond to controls with phase $\Theta=270°$. The total wave number is $K=l=1$ and $R=2000$. (b) Increase in variance for roll perturbations ($k=0$, $\theta=90°$) as a function of the magnitude of the wall normal velocity control for various observation distances $Y_0=0.7$, 0.8, 0.9 from the wall. The bottom curve corresponds to $Y_0=0.7$ and the top to $Y_0=0.9$. The phase of the control is $\Theta=90°$. The total wave number is $K=l=1$ and $R=2000$.

Note the symmetry of response for $\Theta=90°$ and $\Theta=270°$. Symmetry about $\Theta=180°$ can be shown to be a general property of roll perturbation control because the absence of advection in the evolution equations leads to identical energy growth for conjugate controls. Consequently, investigation of control phases $0<\Theta<180°$ exhausts the possibilities.

Despite robust suppression of variance at $\Theta=90°$, it can be seen in Figs. 8(a) and 8(b) that the greatest suppression for roll perturbations occurs at $\Theta=180°$, corresponding to exactly out of phase control. Unfortunately, as we have seen, this out of phase control fails to similarly suppress oblique perturbations because of the existence of an unstable mode. We show in the sequel that $\Theta\approx 90°$ provides the best compromise.

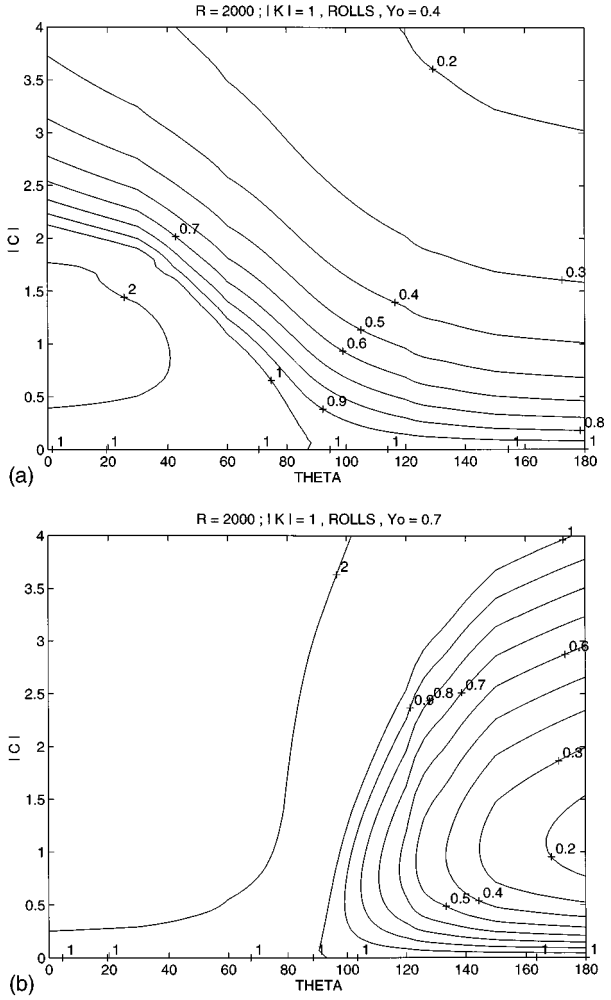

FIG. 8. Suppression of variance for roll perturbations ($k=0$, $\theta=90°$). Shown are contours of $\langle E_c^\infty\rangle/\langle E_0^\infty\rangle$ as a function of the magnitude ($|C|$) and the phase (Θ) of the control. The total wave number is $K=l=1$ and $R=2000$. (a) For observations a distance $Y_0=0.4$ from the walls; (b) for observations a distance $Y_0=0.7$ from the walls.

Understanding the response of roll perturbations to boundary control turns out to be particularly simple. Consider the initial development of a velocity field, which at $t=0$ is confined to a wall normal velocity perturbation $[0,v_0(x,y,z),0]$, with $v_0(x,y,z)$ satisfying the boundary conditions consistent with the control specified by (4). The inviscid evolution, which provides a good initial approximation to the dynamics, satisfies the equations

$$\frac{\partial \Delta v}{\partial t}=0, \tag{19a}$$

$$\frac{\partial u}{\partial t}=-U'v, \tag{19b}$$

$$\frac{\partial \eta}{\partial t}=-U'\frac{\partial v}{\partial y}, \tag{19c}$$

which can be immediately integrated to give

$$v(x,y,z,t)=v_0(x,y,z), \tag{20a}$$

$$u(x,y,z,t)=-v_0(x,y,z)U't. \tag{20b}$$

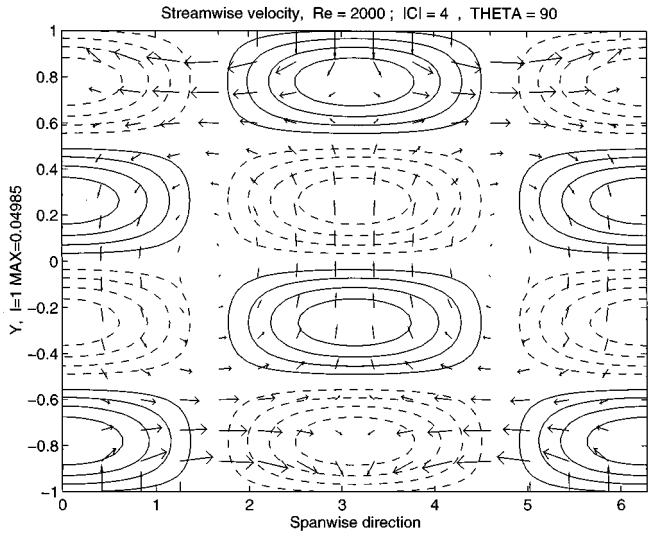

FIG. 9. Contours of streamwise velocity distribution in the $y-z$ plane for the first EOF, which accounts for 52% of the total eddy energy. The perturbations are rolls ($k=0$) with total wave number $K=l=1$. The control has magnitude $|C|=4$ and phase $\Theta=90°$. The variance suppression is 80%. The mean flow is Poiseuille and the Reynolds number is $R=2000$. The plotted vectors are proportional to the projection of the velocity vector on the $y-z$ plane.

$$\eta(x,y,z,t)=-\frac{\partial v_0(x,y,z)}{\partial y}U't. \tag{20c}$$

The fixed structure and linear growth in time of the streamwise streaks is revealed by (20b). The solution does not translate in space and, consequently, control actions for roll perturbations cannot induce superposition and a resulting cancellation of the developing streak. Such superposition cancellation can occur for oblique perturbations leading to enhanced variance suppression. For pure roll disturbances the problem of suppression becomes that of identifying the control parameters that constrain the initial field $v_0(x,y,z)$ in such a way that energy growth is reduced compared to that obtained in the unmanipulated flow. The perturbation energy growth at time t for harmonic perturbations is easily calculated from (20) to be

$$\frac{E(t)}{E(0)}=1+t^2\,\frac{\int_{-1}^{1}dy\;U'^2[d\hat{v}_0(y)/dy]^2}{\int_{-1}^{1}dy\{K^2\hat{v}_0^2+[d\hat{v}_0(y)/dy]^2\}}. \tag{21}$$

The optimal control strategy obtained for controls specified by C,Y_0 is the the one that solves the variational problem:

$$\mathrm{MIN}_{(C)}\;\mathrm{MAX}_{(g)}\left(\frac{\int_{-1}^{1}dy\;U'^2(dg/dy)^2}{\int_{-1}^{1}dy[K^2g^2+(dg/dy)^2]}\right), \tag{22}$$

for all adequately differentiable functions g that satisfy boundary conditions (4) and (6). Solution of this variational problem by standard methods reproduces the variance suppression curves shown in Figs. 8(a) and 8(b)

The first EOF for control amplitude $|C|=4$ and phase $\Theta=90°$ and with observations at a distance $Y_0=0.4$ from the walls is shown in Fig. 9. It is evident that the constraint imposed by the control leads to the development of a much weaker doublet of opposing streaks.

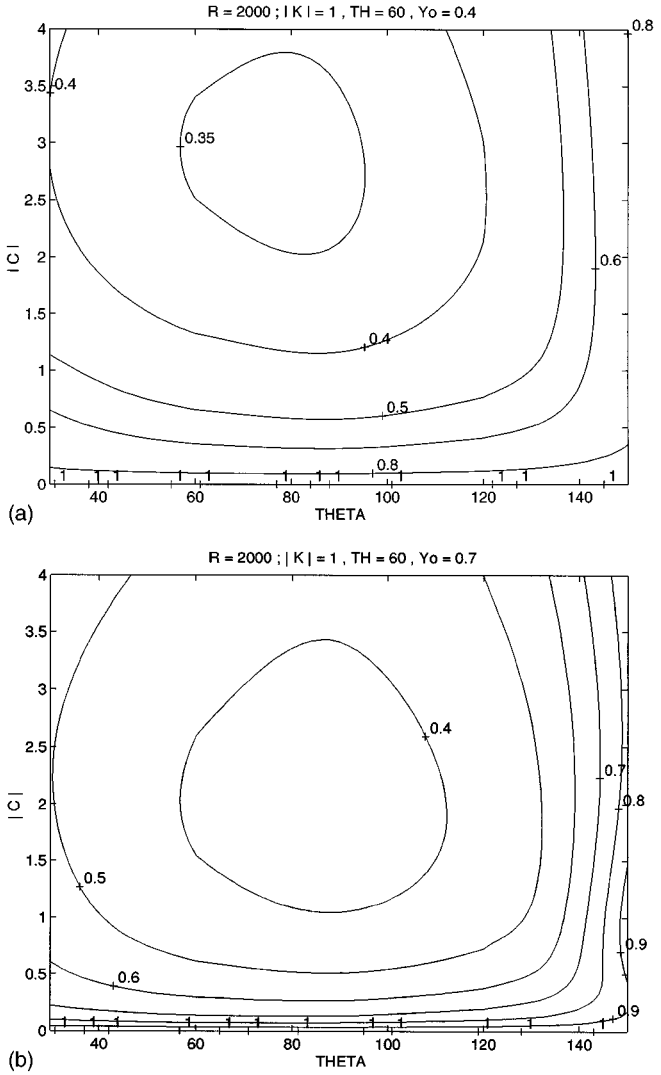

FIG. 10. Suppression of variance as a function of the magnitude ($|C|$) and phase (Θ) of the control for oblique perturbations with $\theta=60°$ [$k=|K|$ cos (θ)]. Shown are contours of $\langle E_c^{\infty}\rangle/\langle E_0^{\infty}\rangle$. The total wave number is $K=1$ and the Reynolds number is $R=2000$. (a) For observations a distance $Y_0=0.4$ from the walls; (b) for observations a distance $Y_0=0.7$ from the walls.

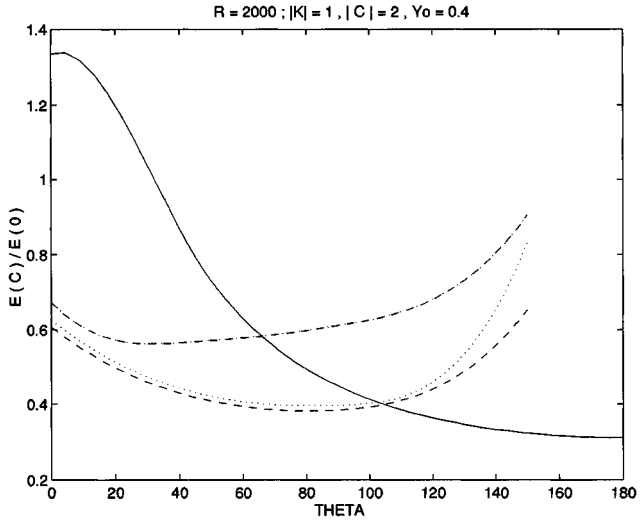

FIG. 11. Suppression of variance as a function of the phase of the control for $|C|=2$ and $Y_0=0.4$ for various perturbations of increasing obliqueness. The continuous curve is for roll perturbations ($\theta=0$). The dashed curve is for an oblique perturbation with $\theta=80°$. The dotted curve is for an oblique perturbation with $\theta=60°$. The dot–dashed curve is for an oblique perturbation with $\theta=0°$. The total wave number is $|K|=1$ and $R=2000$.

V. CONTROL OF OBLIQUE PERTURBATIONS

We turn now to variance suppression for oblique perturbations. A contour plot of the suppression of ensemble-average perturbation energy as a function of the magnitude and phase of the control is shown in Fig. 10(a) for observations located at $Y_0=0.4$ from the wall and in Fig. 10(b) for observations located at $Y_0=0.7$ from the wall. Note that in both cases robust suppression of the order of 60%–70% occurs at $\Theta=90°$. The out of phase and in phase controls are not included in these graphs because they have already been presented in Sec. III. We also have limited our investigation to region $0<\Theta<180°$, although now the advection operator breaks the symmetry about $\Theta=180°$, because the instability of oblique perturbations already evident at $\Theta=180°$ extends to higher values of Θ.

We have already seen that out of phase control suppresses variance optimally for streamwise roll perturbations. However, even slightly oblique perturbations may become unstable for out of phase controls, as can be seen from Fig. 11. Consequently, the most robust strategy is a compromise with control phases in the neighborhood of $\Theta=90°$. We now examine this control strategy in detail.

The suppression of variance for $\Theta=90°$ control for a variety of oblique perturbations with observation at $Y_0=0.4$ is shown in Fig. 12. Note that oblique perturbations, unlike their roll counterparts, exhibit a sharp suppression of variance as the control magnitude increases from zero. In order to understand this behavior consider the stochastic frequency response of the flow. This is obtained by solving for the

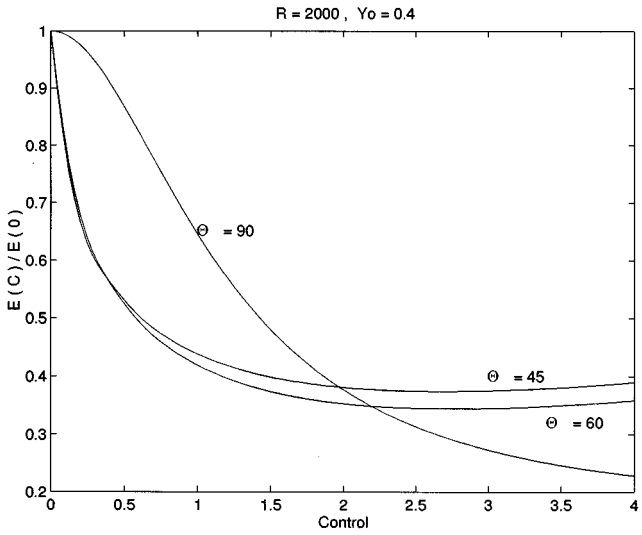

FIG. 12. Suppression of variance as a function of control magnitude for control phase $\Theta=90°$ and $Y_0=0.4$ for various perturbations of increasing obliqueness: $\theta=90°$, 60°, 45°. The total wave number is $K=1$ and $R=2000$.

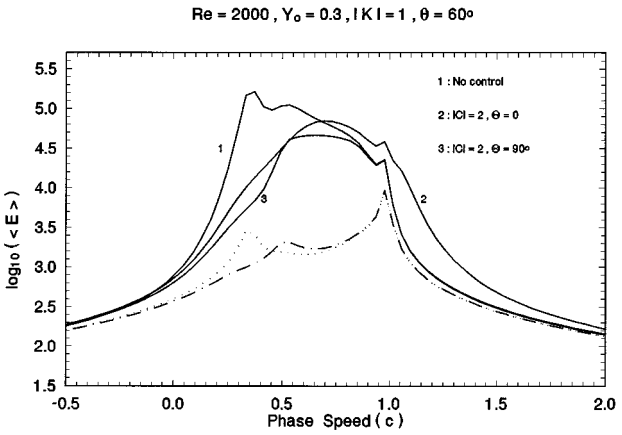

FIG. 13. The energy spectrum produced by white noise forcing as a function of phase speed. Curve 1 corresponds to the response of the unmanipulated flow and the dotted curve is the equivalent normal response. Curve 2 corresponds to an in phase control ($\Theta=0$) of magnitude $|C|=2$. Curve 3 corresponds to control $|C|=2$ at a phase of $\Theta=90°$ and the dot–dashed curve is the equivalent normal response. The total wave number is $K=1$ and $R=2000$.

frequency response of the evolution equation forced by white noise.[18] The ensemble-average energy is given by

$$\langle E^{\infty}\rangle = \int_{-\infty}^{\infty} d\omega \ \mathrm{trace}[\mathscr{R}^{\dagger}(\omega)\mathscr{R}(\omega)], \tag{23}$$

where the dagger denotes the Hermitian transpose and the resolvent is defined as

$$\mathscr{R}(\omega) = (i\omega I - \mathscr{A})^{-1}. \tag{24}$$

The frequency response for $\theta=60°$ perturbations is shown in Fig. 13 for the unmanipulated flow, and for controls with $|C|=2$ and control phases $\Theta=0$, 90. Also plotted is the equivalent normal response calculated as the summation of the residue of the poles of the resolvent, which would give the variance for a normal operator with the same spectrum. Note the profound effect of non-normality in maintaining variance far in excess of what would be anticipated from the rate of dissipation of the modes (this result can be shown to be a necessary consequence of the non-normality of the operator[22]).

It is evident from Fig. 13 that the variance of the controlled flow peaks at higher frequencies corresponding to a shift of the streaks to the interior of the flow where the shear is smaller.

Physically the variance reducing control action inhibits the formation of streaks in the vicinity of the wall where high shear would lead to substantial buildup of streak amplitude. The evolution of the optimal perturbation that grows maximally in ten time units is shown in Figs. 14(a) and 14(b) for the controlled and unmanipulated flow. The control boundary condition induces a time varying cross-stream velocity near the boundaries that inhibits the formation of the energetic near wall streaks. We remark in passing that the most effective cancellation of the near wall streaks by this mechanism would have occurred for out of phase control if there were no instabilities.

Analysis of energetics confirms that the energy growth arising from the Reynolds stress is reduced in the controlled flow [Figs. 15(a) and 15(b)].

An implication of these results is that the rms amplitude of the streamwise and cross-stream velocities in controlled flows peak at greater distance from the wall. This can also be seen to be the case in the numerical simulations presented by Choi *et al.*[20]

VI. DISCUSSION AND CONCLUSIONS

In this work methods for controlling transition to turbulence and suppressing fully developed turbulence have been explored, making use of the theory of stochastically forced non-normal systems. The parametrized turbulent state produced by stochastic forcing of the highly non-normal operator resulting from linearization about the background shear provides a convenient model for testing control strategies. A number of active controls were explored using this model and physical mechanisms by which these controls operate were identified.

This parametrized turbulence accurately models the coherent structures and the energetic interaction of the coherent structures with the mean flow, which sustains the turbulent state. In the form presented in this work this model does not directly provide a theory for the dynamics of the inertial subrange nor for the dynamics of the dissipation range and we defer to extensive previous work under the rubric of isotropic homogeneous turbulence theory that addresses the latter two dynamical regimes. We note in defense of this limitation of our inquiry to the energy bearing scales that the injection of energy mediated by coherent structures is necessary in shear turbulence to supply energy to inertial subrange and ultimately to the dissipation scales.

In the examples examined, the cross-stream velocity was observed at a boundary parallel plane in the interior of the flow, and the surface normal velocity was imposed as a control. Diagnosis of the energy input at the boundary reveals that successful control requires input of energy into the fluid implying that implementation of active control is necessary to obtain turbulence suppression by the mechanisms examined. Examination of Reynolds stress distribution reveals that successful controls reduce the net down-gradient momentum flux by the growing structures sufficiently, to not only compensate for the energy input due to boundary forcing but also to reduce the overall variance. Two mechanisms by which reduction of Reynolds stress is accomplished were identified. One effective means of suppressing perturbations was referred to as overdriving because the effective normal velocity was found to be of large amplitude and in phase with the perturbation normal velocity. This in phase forcing produced the expected destabilization at low driving amplitude, but as the amplitude of the driving was increased the phase of the perturbation was altered to produce decay and suppression of as much as 70% of variance for observations near the wall. The most effective general control resulted from a higher amplitude normal velocity advanced in phase by approximately $\Theta=90°$ compared to the perturbation phase and for observations located near the center of the streak location of the unmanipulated flow. This control also

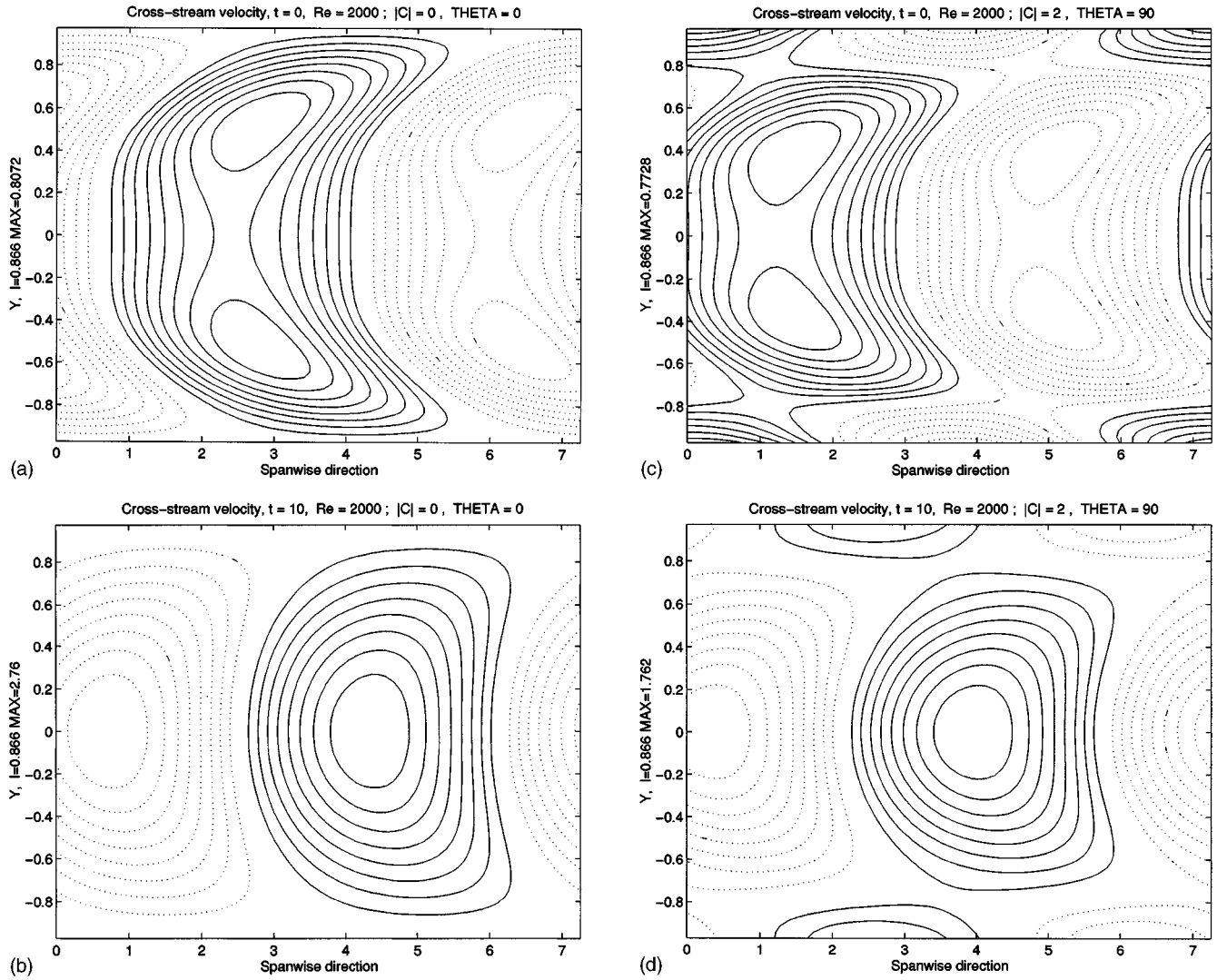

FIG. 14. Evolution of the optimal oblique perturbation with $\theta=60°$ that leads to maximal energy growth in ten units of time for the controlled flow, with $|C|=2$, $\Theta=90°$, and $Y_0=0.3$ and the unmanipulated flow. Compared to the unmanipulated flow there is a 60% variance suppression. (a) Contours of the cross-stream velocity at $t=0$ for the unmanipulated flow. (b) Contours of the cross-stream velocity at $t=10$ for the unmanipulated flow. (c) Contours of the cross-stream velocity at $t=0$ for the controlled flow. (d) Contours of the cross-stream velocity at $t=10$ for the controlled flow. The total wave number is $K=1$ and $R=2000$.

worked by altering the structure of the perturbation so that the down-gradient Reynolds stress was reduced. Out of phase control ($\Theta=180°$) was effective in reducing the variance of almost all perturbations. Unfortunately this promising control gives rise to an instability caused by the boundary control. This instability that occurs for observations $0.3<Y_0<0.7$ limits the practical utility of this control.

Active control has sometimes been referred to as wave cancellation, but this may be misleading because the control, in fact, puts energy into the wave, but in such a way as to modify its structure so that interaction with the mean flow reduces the down-gradient Reynolds stress and in turn reduces the perturbation variance. A more insightful viewpoint is to see the control as an alteration of the boundary condition that more tightly constrains the system and by this means produces a reduction of variance.

Perhaps the most straightforward control to implement would consist in observing the wall pressure and controlling the wall normal velocity. Unfortunately, analysis of the expression for perturbation pressure fluctuations at the wall [Eq. (9)] reveals that the perturbation pressure itself is determined primarily by the wall normal velocity when the mean shear is nonzero at the boundary [first rhs term of (9)]. It follows that perturbation wall pressure in the presence of a mean shear and a wall normal velocity cannot provide an independent observation of disturbances in the interior. It may be possible, however, to offset the observation of pressure from the control either in space or in time to avoid this difficulty.

Reduction of variance by as much as 70% is found for boundary normal velocity control. Prior to transition from laminar flow to turbulence the perturbation field can generally be accurately modeled by the linearized equations because of the smallness of the perturbations, so that the equations used in this work are justified *a priori*. However, in the case of fully developed turbulence, where the rms velocity is

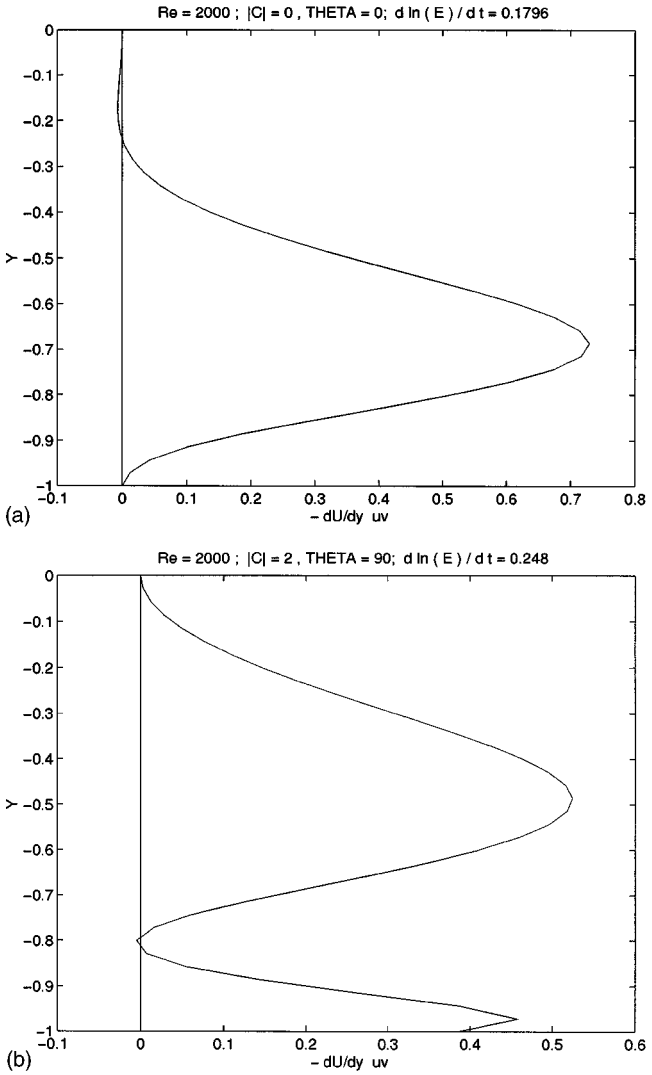

FIG. 15. The energy conversions due to the Reynolds stress term for the optimal disturbances at $t=0$, which are shown in Figs. 14(a) and 14(c), respectively.

of the order of 10% of the mean, linearization entails some loss of accuracy. Nevertheless, we believe that the dominance of the non-normal operator in determining the response of a turbulent flow to both externally and internally generated perturbations justifies the turbulence parametrization used in this work. Efforts are in progress to implement these control strategies in a nonlinear numerical turbulence simulation.

ACKNOWLEDGMENTS

Discussions with Aristotle Arapostathis are gratefully acknowledged.

Petros J. Ioannou was supported by NSF ATM-92-16189. Brian Farrell was supported in part by NSF ATM-92-16813.

[1]D. M. Bushnell, J. N. Hefner, and R. L. Ash, ''Effect of compliant wall motion on turbulent boundary layers,'' Phys. Fluids **20**, 31 (1977). Also, the review article by K. S. Breuer, ''Active control of wall pressure fluctuations in a turbulent boundary layer,'' *ASME Symposium on Flow Noise Modeling, Measurement and Control,* 1993.

[2]L. D. Landau, ''On the problem of turbulence,'' Dokl. AN SSSR **44**, 339 (1944); L. D. Landau and E. M. Lifshitz, *Fluid Dynamics* (Pergamon Press, London, 1963).

[3]W. Wuest, ''Survey of calculation methods of laminar boundary layers with suction in incompressible flow,'' in *Boundary Layer and Flow Control,* edited by G. V. Lachmann (Pergamon Press, New York, 1961), Vol. 2.

[4]A. J. Strazisar, A. J. Reshotko, and J. M. Prahl, ''Experimental study of the stability of heated laminar boundary layers in water,'' J. Fluid Mech. **83**, 225 (1977). Also, refer to H. H. Hu and H. H. Bau, ''Feedback control to delay or advance linear loss of stability in planar Poiseuille flow,'' Proc. R. Soc. London Ser. A **447**, 299 (1994).

[5]M. O. Kramer, ''Boundary layer stabilization by distributing damping,'' J. Am. Soc. Naval Eng. **72**, 25 (1960).

[6]T. B. Benjamin, ''Shearing flow over a wavy boundary,'' J. Fluid Mech. **6**, 161 (1959); M. T. Landahl, ''On the stability of a laminar incompressible boundary layer over a flexible surface,'' *ibid.* **13**, 609 (1962).

[7]H. W. Liepmann and D. M. Nosenchuck, ''Active control of laminar-turbulent transition,'' J. Fluid Mech. **118**, 201 (1982); R. W. Metcalfe, C. J. Rutland, J. H. Duncan, and J. J. Riley, ''Numerical simulations of active stabilization of laminar boundary layers,'' AIAA J. **24**, 1494 (1986); A. S. W. Thomas, ''The control of boundary-layer transition using a wave-superposition principle,'' J. Fluid Mech. **137**, 233 (1983).

[8]H. B. Squire, ''On the stability for three-dimensional disturbances of viscous fluid flow between parallel walls,'' Proc. R. Soc. London Ser. A **142**, 621 (1933).

[9]K. M. Butler and B. F. Farrell, ''Three-dimensional optimal perturbations in viscous shear flow,'' Phys. Fluids A **4**, 1637 (1992).

[10]B. F. Farrell and P. J. Ioannou, ''Optimal excitation of three-dimensional perturbations in viscous constant shear flow,'' Phys. Fluids A **5**, 1390 (1993); ''Perturbation growth in shear flow exhibits universality,'' 2298 (1993).

[11]B. F. Farrell, ''Optimal excitation of perturbations in viscous shear flow,'' Phys. Fluids **31**, 2093 (1988).

[12]L. Boberg and U. Brosa, ''Onset of turbulence in a pipe,'' Z. Naturforshung teil. **43**, 697 (1988).

[13]L. H. Gustavsson, ''Energy growth of three dimensional disturbances in plane Poiseuille flow,'' J. Fluid Mech **224**, 241 (1991).

[14]S. C. Reddy and D. S. Henningson, ''Energy growth in viscous channel flows,'' J. Fluid Mech. **252**, 209 (1993).

[15]L. N. Trefethen, A. E. Trefethen, S. C. Reddy, and T. A. Driscoll, ''Hydrodynamic stability without eigenvalues,'' Science **261**, 578 (1993).

[16]P. J. Schmid and D. S. Henningson, ''A new mechanism for rapid transition involving a pair of oblique waves,'' Phys. Fluids A **4**, 1986 (1992).

[17]B. F. Farrell and P. J. Ioannou, ''Stochastic forcing of the linearized Navier–Stokes equations,'' Phys. Fluids A **5**, 2600 (1993).

[18]B. F. Farrell and P. J. Ioannou, ''Variance maintained by stochastic forcing of non-normal dynamical systems associated with linearly stable shear flows,'' Phys. Rev. Lett. **72**, 1188 (1994).

[19]K. M. Butler and B. F. Farrell, ''Optimal perturbations and streak spacing in wall-bounded turbulent shear flow,'' Phys. Fluids A **5**, 774 (1993).

[20]H. Choi, P. Moin, and J. Kim, ''Active turbulence control for drag reduction wall-bounded flows,'' J. Fluid Mech. **262**, 75 (1994).

[21]D. J. Benney and L. H. Gustavsson, ''A new mechanism for linear and nonlinear hydrodynamic instability,'' Stud. Appl. Math. **64**, 185 (1981).

[22]P. J. Ioannou, ''Non-normality increases variance,'' J. Atmos. Sci. **52**, 1155 (1995).

[23]M. C. Wang and G. E. Uhlenbeck, ''On the theory of Brownian motion II,'' Rev. Mod. Phys. **17**, 323 (1945).

[24]W. C. Reynolds and W. G. Tiederman, ''Stability of turbulent channel flow, with application to Malkus's theory,'' J. Fluid Mech. **27**, 253 (1967).